PHYSICAL REVIEW B VOLUME 27, NUMBER 9 1 MAY 1983

Low-temperature—irradiation study of flux-line pinning in type-II superconductors

H. R. Kerchner, D. K. Christen, C. E. Klabunde, S. T. Sekula, and R. R. Coltman, Jr.
Solid State Division, Oak Ridge National Laboratory, Oak Ridge, Tennessee 37830
(Received 23 December 1982)

Annealed wires of Nb and Nb—20 at. % Ta were irradiated at liquid-helium temperature in two different modes. In one mode thermal neutrons produced 75% of the damage, while in the other mode fast neutrons produced 85% of the damage. The increase in critical current with fluence was measured in order to determine its dependence on pin type and density and material purity. Damage due to the fast-neutron component of the flux dominated the flux pinning in both modes. The observations were consistent with the collective statistical summation theory and inconsistent with the conventional single-particle theory. The elementary pinning interaction deduced from the data by using the collective statistical theory agreed well with a recent theoretical calculation of the interaction due to the electron scattering mechanism.

I. INTRODUCTION

Although critical currents in type-II superconductors have been studied intensively since the early 1960's, a number of fundamental questions about how they arise remain unanswered. The theory of the subject breaks naturally into two parts: (1) the calculation of the elementary interactions between flux lines (FL) and defects and (2) the statistical summation of these interactions to obtain a bulk pinning-force density $-\vec{F}$ that stabilizes the flux-line lattice (FLL) of flux density $\vec{B}$ in the presence of a driving force $\vec{F}=\vec{J}\times\vec{B}$ due to a transport-current density $\vec{J}$. Experimentally it is difficult to isolate one part of the problem because typically only a microstructure characterization and a measurement of the critical- (i.e., maximum-) force density F_c can be made.

Most experiments have been interpreted by using one form or another of the single-particle statistical theory originally due to Labusch.[1] While this theory has had some success when applied to a few experiments, it has not provided a complete understanding of the critical state. The primary difficulties arise from the fact that most crystalline defects are small, and interact only weakly with the FLL. Therefore, they cannot induce the correlations between FL and defect positions that are envisioned in the single-particle theory.

A few years ago Larkin and Ovchinnikov[2] showed theoretically that the FLL in a type-II superconductor is coherent only within a small volume when the superconducting material contains defects. They argued that the small coherent regions must be correlated with the defect array and that one can estimate the FL-pinning-force density in the material by summing the elementary FL-defect interactions within a correlated region using a random-walk argument and dividing the sum by the volume of the region. This estimate can be quite substantial even for arrays of defects that do not interact sufficiently strongly with the FLL to satisfy the "threshold criterion" of the conventional statistical theory.[1] One of the present authors has shown explicitly that the regions described by Larkin and Ovchinnikov are indeed correlated with the defect array, and he has derived a detailed statistical theory.[3]

One expects some materials to obey the new, collective, statistical theory, and others to obey the conventional theory. In principle one can determine which theory is applicable to a given system by calculating the elementary FL-defect interaction. In practice both the experimenal characterization of the defects and the theoretical calculation of the elementary interaction are problematical. Therefore, it is desirable to determine experimentally whether one of the two statistical theories applies to at least a few materials.

Even in the absence of detailed knowledge of the elementary interaction, the applicability of the conventional statistical theory (or some modification of it) or the collective statistical theory should be manifest in the dependence of the critical pinning-force density F_c on the defect-number density n. Strongly

interacting defects should contribute to F_c individually, according to the conventional theory, giving $F_c \propto n$ for small n. Weakly interacting defects can contribute only collectively; the collective theory leads to $F_c \propto n^2$ for small n. While the defect density is typically difficult to control or measure, a low-temperature irradiation provides an ideal means to control n while the intrinsic properties of the material and the character of the individual defects remains constant, at least at low fluences.

A number of radiation-damage experiments have been performed on superconductors, but they have mainly focused on changes in the intrinsic properties of the materials irradiated at relatively high levels of damage. Only two studies can reasonably be used to test the dilute-limit predictions of the two competing statistical summation theories. Berndt *et al.*[4] irradiated niobium with fast neutrons at low temperature (4.6 K) and found $F_c \propto n$ at most values of the magnetic field up to a fluence of 1.4×10^{21} n/m^2 ($n=3.8\times10^{22}$ m^{-3}). At higher fluences, F_c increased less rapidly with fluence. More recently Kupfer and Manuel[5] irradiated V_3Si with fast neutrons at 240 °C and found F_c increased faster than linearly with fluence for low fluences. For the low-temperature irradiation the FL pins are the displacement cascades whose density is just the product of the fluence, the density of atoms in the sample, and the neutron-collision cross section. For the higher-temperature irradiation the FL pins are small point-defect clusters that form as the primary displacement cascade collapses. Although the pin density n can be determined only by transmission-electron-microscope (TEM) examination of the samples, n is known to increase in proportion to fluence up to a fluence of 10^{22} n/m^2 in V_3Si.[5] Thus the results of Ref. 4 obey the conventional statistical-summation theory, while the results of Ref. 5 obey the collective theory.

Although both experiments described above provide some information about FL pinning in the dilute limit, neither is an extensive investigation of this regime. Pinning-force densities are reported in Ref. 4 for only two fluences below 10^{22} n/m^2. An error in just one of these measurements or in the measurement done before the irradiation could change the conclusion. Although the fluence dependence of the results of Ref. 5 are in excellent agreement with the collective theory, that experiment does not adequately test the dilute-limit prediction of the collective theory because F_c was measured at only one fluence in the dilute pinning regime.[3]

We irradiated Nb and Nb—20 at. % Ta wires at 5 K with fast neutrons. Four-terminal measurements of the critical currents were made *in situ* before, during, and after the irradiation in order to obtain the most complete picture possible of pinning by the radiation-induced defects. In the earlier studies the single-crystal samples had to be removed from the reactors and put into a low-temperature magnetometer for measurement. The complexity of this procedure made measurements at more fluences impractical. The present study also differs from the earlier study on Nb in that we measured the critical current before and after irradiation at several temperatures.

While the primary motivation for this experiment was to study the defect-density dependence of the critical current, an important secondary motivation was to compare the FL pinning by the same defects in materials that differ in their electron mean free path and as little as possible in other properties. Dilute alloys of Ta in Nb make an almost ideal system for this comparison. Addition of 20 at. % Ta to Nb lowers the critical temperature T_c from 9.3 K for pure[6] Nb to 8.0 K, while it lowers the mean free path l to 13 nm and increases the Ginzburg-Landau parameter κ from 0.8 for pure[6] Nb to 2.6. Interactions between a FL and a displacement cascade that are associated with the elastic strains in the material or with a variation in T_c within the cascade should not differ greatly between Nb and Nb—20 at. % Ta. On the other hand, if the interaction arises from the additional electron scattering or the increase in κ within the cascade, it may well be substantially different for the two materials because the contrast in κ and l between the displacement cascades and the matrix is much greater in the pure material than in the alloy.

A third goal of the present study was to compare the pinning due to individual Frenkel pairs (produced by recoil from γ emission after a thermal neutron capture) and that due to displacement cascades (produced by fast neutrons). Irradiations were therefore carried out in two modes. In the low-flux mode 75% of the individual displacements were produced by thermal neutrons. In the high-flux mode 85% of the displacements were produced by fast neutrons. Comparing data for both modes made it apparent that all of the observed increase in critical current was due to the fast-neutron damage. Thus, no conclusions could be drawn about pinning by individual Frenkel pairs. All the results will be presented in terms of the fast-neutron fluence.

II. EXPERIMENTAL

A. Sample preparation

The samples were made from zone-refined rods of high-purity Nb and Nb—20 at. % Ta. They were swaged and then drawn to 0.25-mm-diam. wires. It was necessary to anneal the alloy twice during this

process in order to keep it ductile. The wires were heated to 1800 °C for 2 h in 1×10^{-5} Torr oxygen and then annealed at 2200 °C (Nb) and 2300 °C (NbTa) for 4 h in a vacuum better than 2×10^{-9} Torr. Finally, the samples were heated to 400 °C for 4 min in air to oxidize their surfaces. The high-temperature oxygen treatment was intended to remove any carbon introduced into the samples during the swaging and drawing. The vacuum anneal removed the oxygen and other dissolved gases and afforded maximum grain growth. After the anneal the grains were observed to be 3–5 times the wire diameter in length with boundaries perpendicular to the wire axis. Thermal surface oxidation is known to reduce the critical surface current of Nb, which was not of interest in the present study and would only obscure the results. However, the surface oxide causes surface superconductivity to extend to quite high fields. For this reason it was not possible to quench superconductivity entirely in these samples by applying a magnetic field, and accurate measurements of the low-temperature resistance could not be obtained.

In a preliminary run, wires were mounted in the irradiation and measurement apparatus after the heat treatments. Handling and bending the wires to the required 15-mm-diam. loop introduced dislocations that produced an unacceptably high initial critical current. For the subsequent irradiations the samples were formed into loops, leads were attached, and each sample was suspended stress free from a rigid holder before the heat treatments. Then it was not necessary to handle the samples directly in order to mount them in the irradiation and measurement apparatus. The evidence suggests that this precaution practically eliminated the bulk critical-current density leaving only the remaining small critical surface current before the irradiation. A prolate spheroid was spark-machined from a portion of the zoned NbTa rod. It received a high-temperature, ultrahigh-vacuum anneal and a 400 °C oxygen treatment similar to the wires. The equilibrium magnetization and the critical temperature of this sample were measured for use in the analysis of the critical-current data.

B. Experimental apparatus and procedure

The irradiation and the critical-current measurements were carried out in the Oak Ridge National Laboratory low-temperature–irradiation facility, which has been described in detail elsewhere.[7] The apparatus is shown schematically in Fig. 1. A superconducting NbTi solenoid and a pair of samples were mounted in separate, concentric chambers, each of which could be filled with either exchange gas or liquid helium. The magnet chamber was cooled from the outside by circulating liquid helium from a closed-cycle refrigerator that could remove 40 W of heat at 5 K. The sample capsule could be raised and lowered to position the samples individually in the midplane of the solenoid.

The assembly depicted in Fig. 1 was enclosed in a tank filled with D_2O. For operation in the high-flux mode, the reactor core was placed against one face of this tank. For operation in the low-flux mode, a second D_2O tank was inserted between the first one and the reactor. The sample temperature, the flux of thermal and fast neutrons, and the γ-ray heating is shown in Table I for each mode of operation. It was necessary to operate the reactor at one-half of its 2-MW full power in order to reduce γ-ray heating while in the high-flux mode. It will be important to note that the presence of the D_2O in the high-flux mode hardens the fast-neutron spectrum from what it would be if there were no moderator between the reactor and the samples as at the Munich facility where Berndt *et al.*[4] irradiated Nb.

The sample shape was a 240° arc of a 12-mm-diam. circle spot-welded at the ends to two Nb posts mounted on an insulating flange. The sample was supported in the middle by a small loop of Nb wire attached to a tungsten screw. The two Nb posts served as current leads both for the measurements and for annealing each sample. Two 0.25-mm-diam. Nb wires were spot-welded to the sample to serve as voltage leads. (The configuration was slightly different for the preliminary run: The sample was wrapped around an insulating form and was held in place by four NbZr leads spot-welded to it.) For the measurements each sample was situated in the mid-

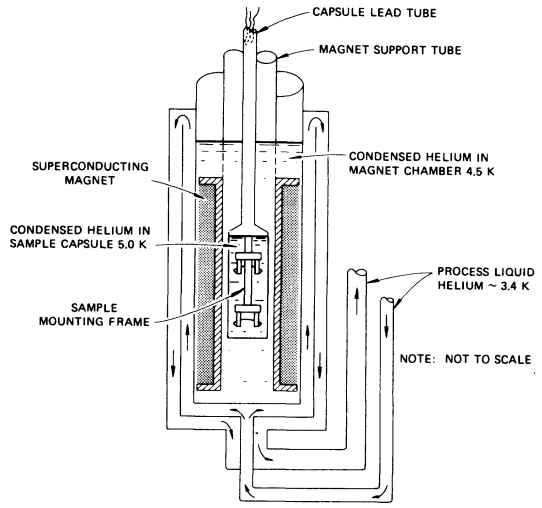

FIG. 1. Schematic representation of the irradiation and measurement apparatus.

TABLE I. Characteristics of the irradiations in the two modes described in Sec. II B. A discussion of the fast-neutron spectrum and the meaning of the flux ϕ_M is given in Sec. II C.

Mode	High flux	Low flux
Sample temperature (K)	5.0	4.5
Thermal-neutron flux ϕ_T (n/m^2 s)	4.3×10^{16}	2.1×10^{16}
Fast-neutron flux ϕ_M (n/m^2 s)	8.8×10^{14}	2.8×10^{13}
ϕ_T/ϕ_M	50	750
γ-ray heating (mW/g)	50	21
Reactor power (MW)	1	2

plane of the superconducting solenoid so that it would be in a uniform, transverse, magnetic field.

For the critical-current measurements the voltage drop across each sample was chopped by using a MOSFET (metal-oxide-semiconductor field-effect transistor) reversing switch,[8] amplified, and detected by a lock-in amplifier. The sample-current supply was programmed by an electronic controller that held the voltage drop across the sample to a preselected value as the magnetic field was swept or stepped through the mixed state. Data were taken both at 1.8 and 0.18 μV for each sample. Since the sample was inductively coupled to the magnet, the field-sweep rate had to be kept low enough that the induced voltage did not appreciably affect the current measurement. Continuous swept-field measurements were easily carried out at 1.8 μV, but the measurements had to be taken point by point at 0.18 μV. The data were recorded by an x-y recorder as plots of critical current I_c vs applied magnetic field H_a.

An example of a recorder plot of I_c vs H_a is shown in Fig. 2. The swept-field measurements show a small field-history effect. This was also present in the measurements at 0.18 μV although only the decreasing-field history is shown. Although the sample current was always larger at 1.8 μV than at 0.18 μV there were no qualitative differences in behavior. For niobium, we took the measurements at 0.18 μV to be representative of the critical state, while for NbTa the 1.8-μV measurements were used. Only the data obtained in decreasing-field history were interpreted. The magnetic flux density β was deduced from measurements of the equilibrium magnetization of a magnetically reversible sample of the same material. Assuming that the current I flowed uniformly throughout the cross-sectional area A of the wire, the force density $F=BI/A$ was calculated.

During the irradiation and for measurements at 3.4 K before and after the irradiation, the samples and magnet were in static columns of liquid helium. Sample temperatures were deduced from measurements of the vapor pressure of the liquid helium in the sample capsule. Measurements on Nb were also carried out at 6.0 K with the sample and the NbTi solenoid in exchange gas. There the sample temperature was deduced from the measured upper critical field. A carbon resistance thermometer served as control sensor for an electronic temperature controller that provided the heat needed to maintain the sample temperature at 6 K. At this temperature the field capability of the NbTi solenoid was not sufficient to investigate NbTa.

Three 7-d irradiations were carried out as follows: In a preliminary run a Nb wire was irradiated in the low-flux mode. Next a new Nb sample and a NbTa

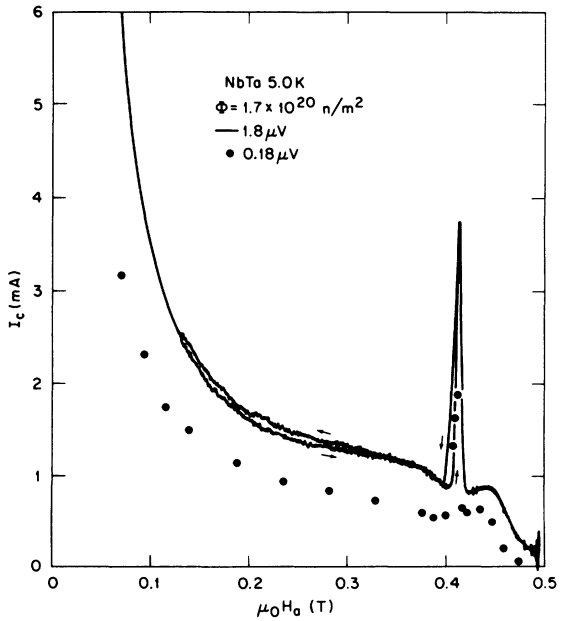

FIG. 2. Critical current I_c of the NbTa wire measured at a voltage criterion of 1.8 μV while sweeping the applied magnetic field H_a. The arrows indicate increasing or decreasing field history. Also shown is the critical current measured point by point at a 0.18-μV criterion in decreasing field. These data were taken with the reactor on after 3 d of irradiation.

sample were irradiated in the low-flux mode. These latter two samples were annealed at room temperature and then irradiated in the high-flux mode. Before and after each irradiation critical-current measurements were made at 3.4, 4.7, and 6.0 K (Nb only). With the reactor on, critical-current measurements were made at the irradiation temperature once or twice each day. Finally, after the last irradiation the samples were annealed 10 min at 50, 100, and 300 K. Critical-current measurements were made at 3.4 K after each anneal.

C. Calibration of the fast-neutron flux

The fast-neutron flux in this facility was determined by seven fast-activation reactions: $^{27}\mathrm{Al}(n,\alpha)^{24}\mathrm{Na}$, $^{46}\mathrm{Ti}(n,p)^{46}\mathrm{Sc}$, and five other (n,p) reactions—$^{47,48}\mathrm{Ti}\rightarrow\mathrm{Sc}$, $^{54,56}\mathrm{Fe}\rightarrow\mathrm{Mn}$, $^{58}\mathrm{Ni}\rightarrow\mathrm{Co}$. Epithermal or "resonance" flux was determined with $^{197}\mathrm{Au}(n,\gamma)^{198}\mathrm{Au}$ (with and without Cd cover). These monitors provided no information over several orders of magnitude of energy below 1.4 MeV. With this rather sparse data none of the existing formal computer codes would be very effective for deducing the spectrum.

Analysis was done assuming that the fast-neutron spectrum could be represented by a fission-spectrum-like peak of Maxwellian form at high energy and a "$1/E$" component at low energy:

$$\frac{d\phi}{dE}=\begin{cases}2\phi_M(A^3E/\pi)^{1/2}e^{-AE}, & E\gg A^{-1}\\ \chi/E, & 0\ll E\ll A^{-1}\end{cases}.$$

The two components must join together smoothly in the vicinity of the peak at $E=(2A)^{-1}$.

The Maxwellian distribution was fitted to the data from the seven fast-activation reactions by integrating the differential flux times cross section for each. The reaction cross-section curves given by Ref. 9 were used. Even at best, the residual variations from detector to detector of the apparent flux ϕ_M exhibited a systematic convex-up curvature when plotted against the response-peak energies of the reactions, indicating that the Maxwellian form is an imperfect representation of the peak. However, the resulting maximum deviations of $\pm 20\%$ were not considered unreasonable. This fit gave $A=0.66$/MeV in the high-flux mode and $A=0.56$/MeV in the low-flux mode. The flux in the peak ϕ_M is quoted in Table I and was used to determine the fast-neutron fluence $\Phi=\phi_M t$ for data analysis. We emphasize that the true fluences are greater than the numbers quoted in this paper by the number of the neutrons in the $1/E$ component. This is a large number of neutrons, but the damage they do contributes little to the pinning-force density. Estimates of the $1/E$ component will be discussed in Sec. III.

The thermal neutron flux was determined in each mode with $^{55}\mathrm{Mn}(n,\gamma)^{56}\mathrm{Mn}$ and $^{59}\mathrm{Co}(n,\gamma)^{60}\mathrm{Co}$ as well as with the gold, and the results are quoted in Table I.

III. THEORY

The conventional, single-particle, statistical-summation theory predicts that the critical-force density F_c is proportional to the defect-number density n and is a complicated function $Q(\delta\Omega)$ of the interaction energy $\delta\Omega$ between a defect and a FL. For several varieties i of defects,

$$F_c=\sum_i n_i Q(\delta\Omega_i)\ . \tag{1}$$

In the present experiment

$$F_c=F_{c0}+\langle Q(\delta\Omega)\sigma_n\rangle n_{\mathrm{Nb}}\Phi\ , \tag{2}$$

where n_{Nb} is the density of the Nb (or NbTa) sample, Φ is the fast-neutron fluence, and F_{c0} is the critical-force density before irradiation. The cross section σ_n is the sum of the cross sections for all damage-producing reactions. The product $Q(\delta\Omega)\sigma_n$ must be averaged over the neutron spectrum and the resulting distribution of cascade sizes.

In contrast the collective-pinning theory predicts

$$F_c=\left[C\sum_i n_i(\delta\Omega_i)^2\right]^2 \tag{3}$$

$$=[F_{c0}^{1/2}+C\langle(\delta\Omega)^2\sigma_n\rangle n_{\mathrm{Nb}}\Phi]^2 \tag{4}$$

for radiation-induced defects. Our results strongly support Eq. (4) and are inconsistent with Eq. (2). This conclusion is most easily verified by examining plots of $F_c^{1/2}$ vs Φ. Therefore, most of the data are presented in this form.

It is of interest to learn what we can about the elementary interaction energy $\delta\Omega$. Evidence will be shown that $\delta\Omega$ is proportional to the number of Frenkel pairs in a cascade. Therefore, the distribution of $\delta\Omega$ values is identical to the distribution of atomic displacements per primary knockon. If this distribution and the constant C were known, the interaction energy per Frenkel pair could be deduced.

The constant C depends on the elastic properties of the FLL and weakly on the detailed characteristics of the defect-FL interaction. The use of a calculation for a simple model interaction[3] enabled us to deduce the sum of the squares of the interaction energies $\langle\delta\Omega^2\sigma_n\rangle n_{\mathrm{Nb}}\Phi$ with an uncertainty of about a factor of 4.

Computer codes based on realistic models of damage production are now available. We have used the code RECOIL[10] to compute the first and second moments of the distribution of atomic displacements D per primary collision for the high-flux mode neutron spectrum. The damage resistivity $\Delta\rho$ is proportional to the total number of atomic displacements (i.e., the first moment),

$$\Delta\rho=[3n_{\mathrm{Nb}}\sigma_{\mathrm{FP}}/2N(0)v_F e^2]\langle D\sigma_n\rangle\Phi \ , \tag{5}$$

where e is the electronic charge, $N(0)$ and v_F are the density of states and velocity at the Fermi surface, and σ_{FP} is an effective electron scattering cross section (the true cross section if the electron scattering were purely s wave). The parameter $\langle\delta\Omega^2\sigma_n\rangle$ deduced from the critical-current measurements is proportional to the second moment of the distribution of displacements,

$$\langle(\delta\Omega)^2\sigma_n\rangle=(\delta\Omega_{\mathrm{FP}}^2)\langle D^2\sigma_n\rangle \ , \tag{6}$$

where $\delta\Omega_{\mathrm{FP}}$ in the FL interaction energy per Frenkel pair. Then

$$\frac{\delta\Omega_{\mathrm{FP}}}{\sigma_{\mathrm{FP}}}=\frac{3n_{\mathrm{Nb}}}{2N(0)v_F e^2}\frac{\langle D\sigma_n\rangle}{\langle D^2\sigma_n\rangle^{1/2}}\frac{\langle(\delta\Omega)^2\sigma_n\rangle^{1/2}}{\Delta\rho/\Phi} \ . \tag{7}$$

The computations yielded $\langle D\sigma_n\rangle/\langle D^2\sigma_n\rangle^{1/2}=2.0\times10^{-14}$ m for Nb and 2.2×10^{-14} m for Nb–20 at. % Ta.

In order to carry out the numerical computations we estimated the flux in the $1/E$ component of the neutron spectrum. Several estimates can be made. Examination of some well-characterized reactor-fast-neutron spectra shows a nearly level region between 0.1 and 1 or 2 MeV in a plot of $E\,d\phi/dE$ vs E. If that is true of this facility then the total fast flux is $\phi(E>0.1\ \mathrm{MeV})=1.7\times10^{15}\ n/\mathrm{m}^2\,\mathrm{s})$, of which 42% is at $E>1$ MeV. This is the highest estimate. About half as much $1/E$ component results from another assumption, namely that this component should match the top of the peak in the $d\phi/dE$ vs E representation. In that case the total $\phi(E>0.1$ MeV$)=1.3\times10^{15}\ n/\mathrm{m}^2\,\mathrm{s}$, of which 52% is above 1 MeV. A lower-limit estimate results from the assumption that the measured Au activation due to the resonance peak at 5 eV establishes a coefficient for the $1/E$ flux which applies all the way up to the fast peak. In that case there would be about $\frac{1}{7}$th as much $1/E$ flux as in the first estimate and the resulting total would be 1.0×10^{15} of which 73% would be above 1 MeV. The correct value probably lies between the first two estimates. The largest estimate was used for the computations. With this estimate two-thirds of the atomic displacements were produced by neutrons having energies greater than 1 MeV. This component of the spectrum is reasonably well determined. The second estimate would give about 17% fewer displacements and would decrease $\langle D^2\sigma_n\rangle$ by a smaller amount. Thus, we can expect that the calculated values of $\langle D\sigma_n\rangle/\langle D^2\sigma_n\rangle^{1/2}$ are upper limits, but that they are not likely to be more than 17% too high.

Since it was not possible to obtain good measurements of the damage resistivity $\Delta\rho$ in our samples, we estimated $\Delta\rho$ by using the results of previous studies. The damage rate $d\rho/d\Phi_f$ for a pure ^{235}U fission spectrum was previously measured for both Nb and Cu.[11] The damage rate in Cu due to the fast neutrons in the high-flux mode is the measured total damage rate in this mode[12] less the measured rate of thermal neutron damage.[13] The desired fast-neutron damage rate in Nb we estimated to be larger than the fission-spectrum damage rate in proportion to the ratio of the two damage rates in Cu. This procedure gave $d\rho/d\Phi=6.4\times10^{-31}\ \Omega\,\mathrm{m}^3/n$.

For a displacement cascade of any size, the ratio of its FL pinning energy to its effective s-wave electron scattering cross section is given by Eq. (7).

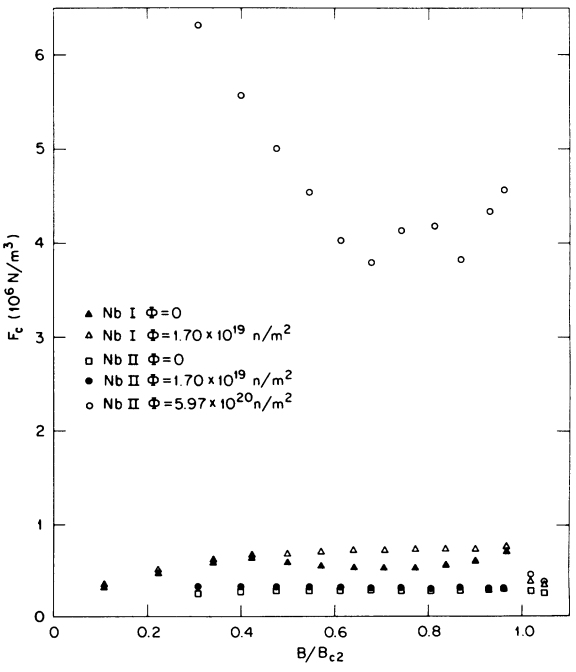

FIG. 3. Measured critical-force density F_c plotted vs reduced flux density B/B_{c2} for the two Nb samples. The voltage criterion for determining critical current was 0.18 μV. The fast-neutron fluence of $1.70\times10^{19}\ n/\mathrm{m}^2$ was attained in the low-flux mode, while $5.97\times10^{20}\ n/\mathrm{m}^2$ was reached in the high-flux mode. The method of counting neutrons is discussed in Sec. II C.

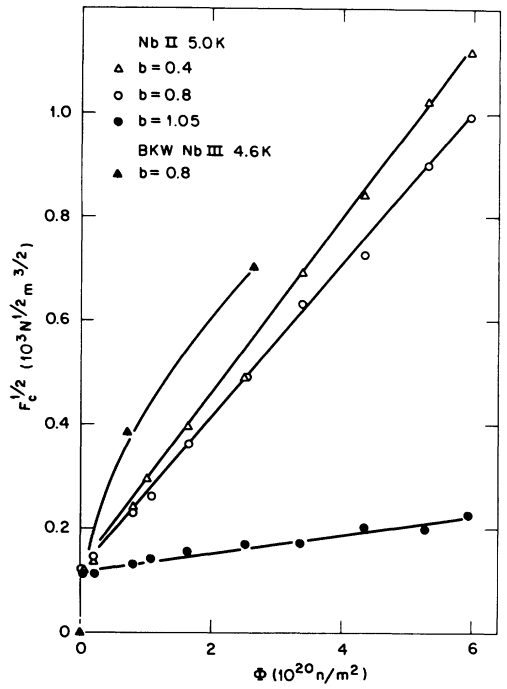

FIG. 4. Increase in $F_c^{1/2}$ with fast-neutron fluence is shown at three reduced flux densities $b=B/B_{c2}$ for Nb II at the irradiation temperature $T=5.0$ K. The comparable results reported by Berndt, Kartascheff, and Wenzl (BKW Nb III) (Ref. 4) are shown for comparison. Our method of counting neutrons is described in Sec. II C.

This ratio will be compared with the result of microscopic theory below.

IV. RESULTS

A. Niobium

The critical pinning-force density F_c is shown in Fig. 3 for the niobium samples at 3.4 K as prepared and after each irradiation. Initially the apparent F_c of Nb II was small and nearly independent of B. The near absence of structure at the upper critical field suggests that the observed critical current was mostly a near-surface effect and was not due to bulk pinning. Irradiation in the low-flux mode increased the critical current of this sample only slightly. Nb I showed a sharp drop in F_c at the upper critical field both before and after irradiation as did Nb II after irradiation. These latter three curves had peaks for B just below the flux density B_{c2} at the upper critical field and for $B \leq 0.4B_{c2}$.

The increase in F_c as a function of fast-neutron fluence Φ (counting only neutrons in the Maxwellian peak as discussed in Sec. II C) is shown in Fig. 4 at two values of the reduced flux density $b=B/B_{c2}$ in the mixed state. For comparison the much smaller increase just above the upper critical field is also shown. These data were obtained during the irradiation with the reactor on. In the mixed state the results firmly establish a linear proportionality between $F_c^{1/2}$ and Φ. Above B_{c2} the increase in critical current is not sufficient to discriminate between Eqs. (2) and (4).

The measurements reported by Berndt *et al.*[4] at $b=0.8$ are also shown in Fig. 4. Before irradiation their sample was extremely reversible so that F_{c0} was nearly zero. Their data fall close to the $\Phi^{1/2}$ curve shown and thus imply qualitatively different behavior than do our data. Some possible reasons for this discrepancy between the two experiments will be discussed in Sec. V. Note that the neutron spectra and methods of counting neutrons are different for the two experiments, and the horizontal axis should be regarded as arbitrary when comparing them.

Equation (4) makes a prediction for the annealing behavior of F_c if one knows the dependence of $\delta\Omega$ on the number of Frenkel pairs within a displacement cascade. Here we assume the simplest reasonable dependence: $\delta\Omega$ is proportional to the number of pairs. Since the damage resistivity $\Delta\rho$ is a good measure of the total number of Frenkel pairs in the sample,

$$n_{\mathrm{Nb}}\langle\delta\Omega\,\sigma_n\rangle\Phi \propto \Delta\rho \ . \tag{8}$$

During the irradiation the distribution of $\delta\Omega$ should remain constant so that

$$\Delta(F_c^{1/2}) \equiv F_c^{1/2} - F_{c0}^{1/2} \propto \Delta\rho \ . \tag{9}$$

After the irradiation is completed, low-temperature annealing permits interstitials to migrate to nearby vacancies and annihilate reducing $\Delta\rho$ and each $\delta\Omega$. Then

$$\Delta(F_c^{1/2}) \propto (\Delta\rho)^2 \tag{10}$$

by Eqs. (4) and (8). This behavior, indicated by the solid lines with arrows in Fig. 5, is confirmed by the data.

It should be noted that the measurements made after annealing were performed at a lower temperature than those made during the irradiation. For this reason $\Delta F_c^{1/2}$ was normalized by its value after the irradiation in the high-flux mode so that the two sets of measurements could be compared on the same graph. Also we emphasize that we did not measure the damage resistivity. Instead $\Delta\rho$ was estimated from the results of previous annealing studies of similar niobium samples.[14] Having to estimate $\Delta\rho$ reduces the precision of the results.

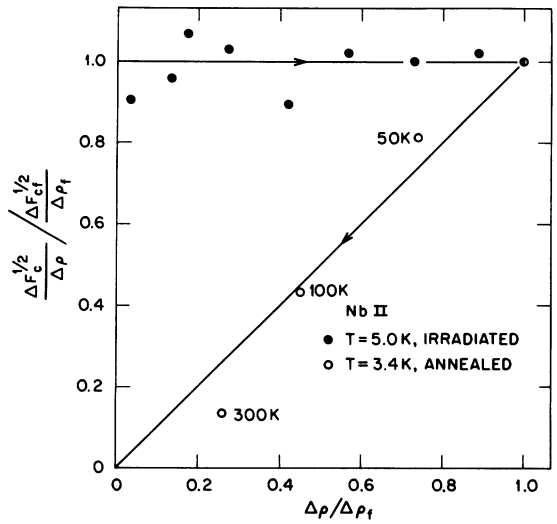

FIG. 5. Normalized increase in $F_c^{1/2}$ divided by the damage resistivity during the irradiation at 5 K and after annealing at three temperatures is shown for Nb II at the reduced flux density $b=0.4$. The lines with arrows indicate the expected behavior.

Nevertheless, the simple picture described above is amply confirmed by the data.

Comparing the two Nb samples having different initial critical currents further tests Eq. (4). In Fig. 6 the increases in $F_c^{1/2}$ during the irradiation in the low-flux mode are shown. Although the increase in F_c is too small to verify $F_c^{1/2} \propto \Phi$ in these data the rates of increase of $F_c^{1/2}$ with Φ can be compared. The lines drawn through the data have the same slope as predicted by Eq. (4). Since the Nb I data were obtained at a slightly lower temperature, one expects $F_c^{1/2}$ to increase more rapidly with irradiation for Nb I than for Nb II. Indeed the data show evidence of a small difference in the slopes $dF_c^{1/2}/d\Phi$ of the two samples.

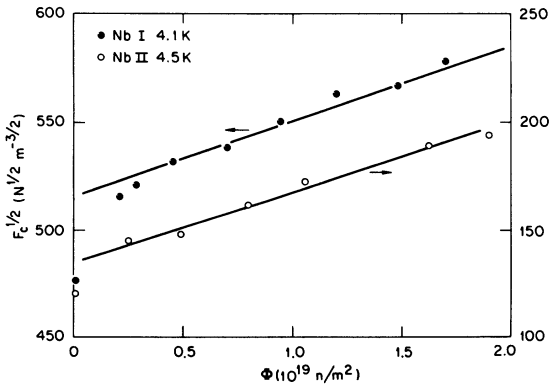

FIG. 6. The increases in $F_c^{1/2}$ with fast-neutron fluence for the two Nb samples are compared at the reduced flux density $b=0.7$. These data were obtained in the low-flux mode. The method of counting neutrons is discussed in Sec. II C.

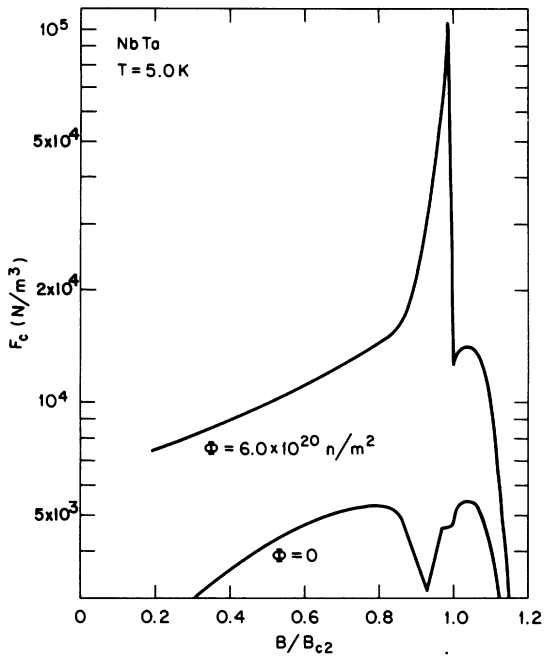

FIG. 7. Measured critical-force density F_c of the Nb–20 at. % Ta sample before and after irradiation in the high-flux mode. The voltage criterion for determining critical current was 1.8 μV. The method of counting neutrons is discussed in Sec. II C.

Of more concern is the fact that the first measurements lie well below the extrapolation to $\Phi=0$ of the large-Φ data. This effect is more pronounced for Nb I. One would be tempted to throw out these first points were it not for the fact that the measurements made with the reactor off before and after the irradiation tend to support the results shown in Fig. 6. There is apparently some mechanism more important at very low fluences than that assumed in the derivation of Eq. (4).

B. NbTa

The NbTa sample showed only a very small increase in critical current with irradiation in the low-flux mode. Those data will not be discussed. The results at 3.4 K before and after irradiation in the high-flux mode are shown in Fig. 7. Both the critical-current and the critical-force density are well below the values for the unirradiated Nb II. Before irradiation F_c shows unusual structure just below and just above the upper critical field. The force density increases about a factor of 2 with irradiation except within a narrow peak above $B=0.85B_{c2}$.

This peak first appears on the shoulder at $B=0.98B_{c2}$, then it grows rapidly wiping out the structure below B_{c2} present before irradiation.

The structure in F_c before irradiation almost certainly arises due to sample inhomogeneity. It is likely that Nb evaporated preferentially from the wire surface during the anneal leaving behind a Ta-rich, near-surface region with higher κ and B_{c2} than the bulk. The large peak effect apparently is associated with the bulk, while the small peak at $B=1.04B_{c2}$ must be due to a high-κ region. One can speculate that before irradiation F_c in the bulk peaks at $B=0.8B_{c2}$ and falls to zero at B_{c2}. Above $B=0.93B_{c2}$ the observed current flows in the near-surface region where F_c peaks at $B=1.04B_{c2}$. (Here B_{c2} is the value measured on the prolate spheroid cut from the same zoned rod that was used to prepare the wire.)

The increase of $F_c^{1/2}$ with fast-neutron fluence is shown in Fig. 8 at the peak ($b=0.99$), on the low-field side of the peak ($b=0.96$), and at two smaller values of the reduced flux density b. The small increase in F_c at small b makes it impossible to demonstrate conclusively either linear or quadratic Φ dependence, but the data fit Eq. (2) better than

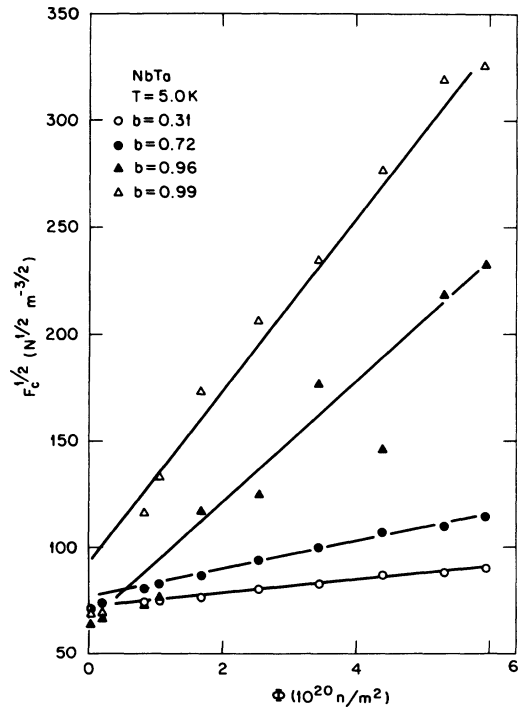

FIG. 8. Increase in $F_c^{1/2}$ with fast-neutron fluence is shown at four reduced flux densities for the Nb—20 at. % Ta sample at the irradiation temperature $T=5.0$ K. The method of counting neutrons is discussed in Sec. II C.

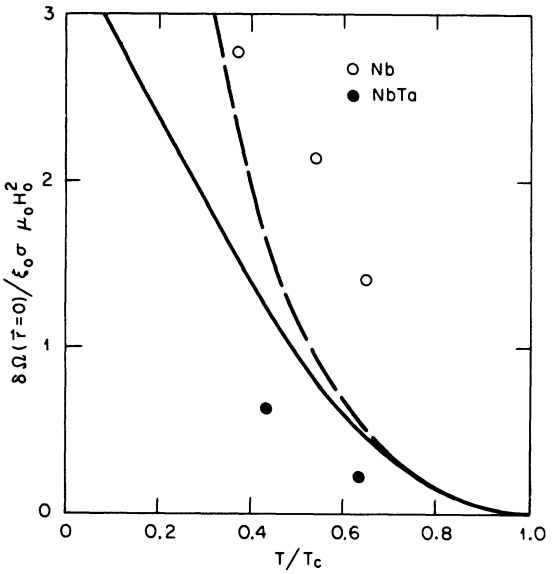

FIG. 9. Pinning-interaction energy $\delta\Omega(\vec{r}=0)$ between an isolated flux line and a displacement cascade, deduced from the data by using the theoretical results of Ref. 3, is compared with the calculation of Ref. 15 in the weak-scattering limit (dashed line) and the unitary limit (solid line). The values of $\delta\Omega$ for both materials were normalized to the indicated product of the BCS coherence length ξ_0, the electron scattering cross section σ, and the square of the zero-temperature critical field H_0 for Nb, calculated as described in the text.

Eq. (4). On the other hand, the growth of the peak is clearly faster than linear in Φ and fits Eq. (4) adequately. Again, if we assume that Eq. (4) applies to the higher fluences, then we must conclude that there is some other effect dominant at the lowest fluences.

C. The elementary interaction

Since the weight of the evidence clearly supports the collective pinning theory, it is reasonable to apply this theory to deduce the mean-square interaction energy $\delta\Omega$ between a FL and a displacement cascade. Specifically, the main results, Eqs. (44) and (51) of Ref. 3, were fitted to the Nb data at 3.4, 5.0, and 6.0 K and to the NbTa data at 3.4 and 5.0 K after irradiation to 6×10^{20} n/m^2. (All results were corrected for the preirradiation F_c.) The parameter α of Ref. 3 is just $\alpha=\delta\Omega/\mu_0 H_c^2$. A minimum bundle size of $N=40$ FL fitted all of the results near B_{c2} satisfactorily.

The values of $\delta\Omega/\sigma$ deduced from the data by using Eq. (7) are compare in Fig. 9 with the recent theoretical calculations of Thuneberg, Kurkijärvi, and Rainer.[15] The theory describes the pinning in-

teraction due to electron scattering by a defect. A clean superconducting matrix and s-wave scattering are assumed. The BCS coherence length ξ_0 and the zero-temperature critical field H_0 for Nb were used in the normalization for both materials. The interaction is clearly smaller in NbTa than in Nb but the results for both materials are in reasonable agreement with the theory.

Because 90% of $\langle n(\delta\Omega)^2 \rangle$ arises from values of $\delta\Omega < \frac{1}{2}\mu_0 H_c^2 \xi^3$, the deduced values of $\delta\Omega$ are small enough to be consistent with the assumption that the collective statistical summation should apply. On the other hand, $\xi_0\sigma$ is about 7 times the cascade volume, making the interactions deduced from the data much stronger than estimates based on known mechanisms other than that of Ref. 15.

V. DISCUSSION AND CONCLUSIONS

A. Fluence dependence

The experimental results described in the last section are clearly inconsistent with the conventional, single-particle, statistical-summation theory as summarized by Eqs. (1) and (2). They show satisfactory consistency with the collective theory as summarized by Eqs. (3) and (4). The confirmation of Eq. (4) is most striking precisely where it is most likely to fail. One might expect the displacement cascades to interact sufficiently strongly with the FLL that the conventional theory should apply. Then the force density would be equal to the product of the density of cascades and the maximum interaction force of each in order of magnitude—much larger than the force density resulting from collective effects. But it is the largest increase in F_c that is most clearly quadratic in defect density. All of the data must be evaluated with this observation in mind.

There are several sets of observations where the fluence dependence of F_c is more nearly consistent with Eq. (2) than Eq. (4). This is true of the results for NbTa at most fields and of the results obtained in the low-flux mode. In view of the clear confirmation of the collective theory by the results obtained on Nb II in the high-flux mode, it makes no sense to apply the conventional theory to these other results. Also we emphasize that any conclusions drawn from the smaller increases in F_c are less certain than those drawn from larger increases. Nevertheless, several observations are significantly inconsistent with Eq. (4) and require some explanation. In the following we offer two speculations as to the reasons for these results.

First, a simple spurious effect could have produced the observed deviations from Eq. (4). This effect arises from inhomogeneity in F_c, which was manifest in the nonlinear current-voltage relations we observed. A nonuniform F_c before irradiation was expected for Nb II and NbTa because the annealing temperature was not uniform over the gauge length of these samples. (The voltage leads were significant heat sinks.) Presumably the entire voltage drop was concentrated in the section of wire where the highest annealing temperature was reached, about midway between the voltage leads. Since F_c increased nonlinearly with fluence, the length of this region of sensitivity must have changed during the irradiation. Assuming that Eq. (4) holds at every point in the wire, one can deduce that the current measured at constant voltage will increase less than linearly with fluence at first. This effect disappears as F_c becomes large compared with F_{c0}.

Second, measurements above the upper critical field revealed that the sample surface carried a significant current that increased with neutron fluence. There is no reason to suppose that this surface pinning should obey Eq. (4). Indeed, collective FL pinning in superconducting films leads to linear proportionality between F_c and n.[2] The existence of a contribution to I_c that is linear in fluence also leads to apparent deviations from Eq. (4) which are similar to those observed.

The discrepancy between the present results and those reported by Berndt *et al.* are difficult to understand. It seems to imply that different statistical summation theories apply to the two experiments. This situation would be credible if their irradiation produced larger displacement cascades than ours. In fact the opposite is expected because the neutron spectrum is harder (in the high-flux mode) in the Oak Ridge facility than at Munich.

An important difference between the two experiments is that Berndt *et al.* measured the magnetization of a cylindrical sample in an axial field while we measured the current in a cylindrical sample in a transverse field. Both measurements give the critical-force density by elementary arguments. However, the magnetization is much more sensitive to errors of interpretation due to surface pinning and uncertainties in the measurement than is our more direct technique. Both problems are especially troublesome at low fluences where the magnetic hysteresis is only a small portion of the total magnetization. The best guess we can make to explain the discrepancy between the two experiments is that one or more of the measurements reported in Ref. 4 for the lowest fluences was in error. The critical-force density deduced may also have been influenced by their neglect of surface hysteresis. We emphasize that this criticism of the results of Berndt *et al.* pertains only to their first few measurements at low flu-

ences and not to the main body of their observations which were made at much higher fluences and involved much larger effects.

B. Elementary pinning interaction

By using the theoretical results of Ref. 3, the ratio of the elementary interaction energy $\delta\Omega$ to the electron scattering cross section σ has been deduced from the data, and the results compare favorably with the microscopic theory of Ref. 15, which describes pinning by the electron scattering mechanism. The interaction energy is quite large and is substantially different for the two materials.

The theoretical calculation[15] applies to the clean limit and no prediction is made for the purity dependence. Recently Yetter *et al.*[16] have used a classical argument to calculate the pinning interaction by the electron scattering mechanism for materials of arbitrary purity. Their result apparently is wrong in the clean limit, where it goes to zero in contradiction to the microscopic theory. Nevertheless the data obtained by Thomas[17] on oxygen-doped Nb foils and the data obtained by Talvacchio[18] on Nb_3Sn films are in agreement with their prediction that the interaction should increase with impurity content for values of the impurity parameter $\alpha=0.88\xi_0/l$ in the range 0.03 to 10. Our two materials are also in this range but show that the pinning interaction decreases with increasing α.

An extension of the microscopic theory to impure materials, coupled with additional experimental investigations of the purity dependence of FL pinning, is needed to clarify our understanding of the electron scattering mechanism.

C. Conclusions

The present experimental study of FL pinning by radiation-induced damage provides the first direct and convincing confirmation of the collective statistical-summation theory in bulk materials. This theory, although very approximate in its present form, agrees with the data in substantial detail. The predicted quadratic dependence of F_c on n is clearly and reliably demonstrated. With somewhat less confidence, the quartic dependence of F_c on $\delta\Omega$ and the simple rule for summing the pinning interactions of different types of defects have been confirmed.

With the use of the collective statistical-summation theory, the elementary pinning interactions in the two materials investigated have been deduced. These results are substantially in agreement with a recent calculation based on the microscopic theory of pinning by the electron scattering mechanism. The present study is one of the very rare instances where a nearly complete quantitative understanding of the critical state has been achieved.

ACKNOWLEDGMENTS

We gratefully acknowledge the assistance of J. F. Emery in making the neutron activation measurements. We are also grateful to M. T. Robinson for helpful advice and discussions. This research has been sponsored by the Division of Materials Science, U. S. Department of Energy, under Contract No. W-7405-eng-26 with the Union Carbide Corporation.

[1]R. Labusch, Cryst. Lattice Defects 1, 1 (1969); A. M. Campbell, Philos. Mag. B 37, 149 (1978).

[2]A. I. Larkin and Yu N. Ovchinnikov, J. Low Temp. Phys. 34, 409 (1979).

[3]H. R. Kerchner, J. Low. Temp. Phys. 50, 337 (1983).

[4]H. Berndt, N. Kartascheff, and H. Wenzl, Z. Angew. Phys. 24, 305 (1968).

[5]H. Küpfer and A. A. Manuel, Phys. Status Solidi A 54, 153 (1979).

[6]H. R. Kerchner, D. K. Christen, and S. T. Sekula, Phys. Rev. B 21, 86 (1980).

[7]C. E. Klabunde, J. M. Williams, and R. R. Coltman, Jr., J. Nucl. Mater. 99, 294 (1981).

[8]The technique is similar to that described in Ref. 6. For this experiment, the transistor switches could not be placed in the cryostat because they would suffer radiation damage. Instead they were mounted in a thermally shielded enclosure so that the thermal emf would be stable and could be canceled.

[9]D. I. Garber and R. R. Kinsey, Brookhaven National Laboratory Report No. BNL-325, 3rd ed. (unpublished).

[10]T. A. Gabriel, J. D. Amburgey, and N. M. Greene, Oak Ridge National Laboratory Report No. ORNL/TM-5160 (unpublished); Nucl. Sci. Eng. 61, 21 (1976).

[11]J. B. Roberto, C. E. Klabunde, J. M. Williams, R. R. Coltman Jr., M. J. Saltmarsh, and C. B. Fulmer, Appl. Phys. Lett. 30, 509 (1977).

[12]R. R. Coltman, Jr. and C. E. Klabunde (unpublished).

[13]R. R. Coltman, Jr., C. E. Klabunde, J. K. Redman, and A. L. Southern, Radiat. Eff. 16, 25 (1972).

[14]J. B. Roberto, C. E. Klabunde, J. M. Williams, and R.

R. Coltman, Jr., J. Nucl. Mater. 73, 97 (1978).
[15]E. V. Thuneberg, J. Kurkijärvi, and D. Rainer, Phys. Rev. Lett. 48, 1853 (1982).
[16]W. E. Yetter, D. A. Thomas, and E. J. Kramer, Philos. Mag. B 46, 523 (1982).
[17]D. A. Thomas, Ph.D. thesis, Cornell University, 1981 (unpublished).
[18]John Talvacchio, Ph.D. thesis, Stanford University, 1982 (unpublished).